Med Ultrason 2013, Vol. 15, no. 3, 184-190
DOI: 10.11152/mu.2013.2066.153.dmm1vg2

Computer aided diagnosis method for steatosis rating in ultrasound images using random forests

Dan Mihai Mihăilescu[1], Vasile Gui[1], Corneliu Ioan Toma[1], Alina Popescu[2], Ioan Sporea[2]

[1]Department of Telecommunications, Faculty of Electronics and Telecommunications, "Politehnica" University, [2]Department of Gastroenterology and Hepatology, "Victor Babeş" Medicine and Pharmacy University Timişoara, Romania

Abstract

In this paper we discuss the problem of computer aided evaluation of the severity of steatosis disease using ultrasound images, **the aim of** the study being to compare the automatic evaluation of liver steatosis using random forests (RF) and support vector machine (SVM) classifiers. **Material and method:** One hundred and twenty consecutive patients with steatosis or normal liver, assessed by ultrasound by the same expert, were enrolled. We graded steatosis in four stages and trained two classifiers to rate the severity of disease, based on a large set of labeled images and a large set of features, including several features obtained by robust estimation techniques. We compared RF and SVM classifiers. The classifiers were trained using cross-validation. There was 80% of data randomly selected for training and 20% for testing the classifier. This procedure was performed 20 times. The main measure of performance was the accuracy. **Results:** From all cases, 10 were rated as normal liver, 70 as having mild, 33 moderate, and 7 severe steatosis. Our best experts' ratings were used as ground truth data. RF outperformed the SVM classifier and confirmed the ability of this classifier to perform well without feature selection. In contrast, the performance of the SVM classifier was poor without feature selection and improved significantly after feature selection. **Conclusion:** The ability and accuracy of RF to classify well the steatosis severity, without feature selection, were superior as compared to SVM.

Keywords: steatosis, ultrasound image, computer aided design, robust methods, classifier, noninvasive

Introduction

Steatosis is one of the most prevalent liver diseases worldwide encountered, especially in developed countries. The main feature of steatosis is the accumulation of fat tissue (usually triglycerides) within liver cells, as a result of malfunctions in liver metabolic processes. A common reason of this malfunction is the alcohol consumption on a regular base. However, steatosis is also frequent in non-alcoholic patients. This kind of steatosis is named nonalcoholic fatty liver disease (NAFLD) [1] and can be caused by a variety of metabolic disorders, such as obesity, diabetes, rapid weight loss, etc.

Received 01.06.2013 Accepted 30.06.2013
Med Ultrason
2013, Vol. 15, No 3, 184-190
Corresponding author: Alina Popescu
8 Barbu Iscovescu str, Sc. A, Ap. 7
300561 Timişoara, Romania
Tel: 0748331233, Fax: 0256488003
Email: alinamircea.popescu@gmail.com

NAFLD represents a broad range of conditions, starting from simple steatosis, which usually follows a benign and stable clinical stage, and ending with the nonalcoholic steatosis, with a high risk of progress to cirrhosis and hepatocellular carcinoma (HCC). Steatosis is also commonly found in histological specimens from patients infected with hepatitis virus C (HCV) being considered an additional risk factor for these patients [2] due to its association with fibrosis progression.

Early detection of steatosis, as well as evaluation of the progression or regression of the disease during medical treatment are important. The most accurate test for steatosis assessment is the liver biopsy. This is a highly invasive procedure, associated with risks, given that a tissue sample from the liver is extracted. Additionally, the liver biopsy results may be affected by sampling errors and interobserver variability [3]. Therefore a safe practice is to use the golden standard liver biopsy only when noninvasive methods fail.

Advanced biomedical imaging techniques available today have been widely used in order to detect and evaluate steatosis. A computed tomography (CT) study [4], reported reliable results, with sensitivity of 82% and specificity of 100% of the method in steatosis evaluation. The comprehensive study of Bohte et al [5] revealed that magnetic resonance imaging, (MRI) outperforms, CT in the diagnosis and quantification of steatosis. However, given the inherent exposure to ionizing radiation and the high costs, CT and MRI should be used with caution, especially in children.

In contrast with CT and MRI, ultrasound (US) imaging is a completely noninvasive method for evaluation of the liver. Also, US has a low cost making this method suitable for screening and progression evaluation during treatment.

The performances of US steatosis evaluation studies vary largely in the literature, probably due to the occurrence of concomitant liver pathology which may affect the liver image. Fibrosis, for example, is also hyperechoic and may or may not coexist with steatosis. Additionally, the visual perception of brightness and colors is known to be relative. While this feature is, most of the time, useful in life, it often makes medical image analysis a challenging task. In spite of the superior intelligence and experience of experts performing visual analysis of US images, the results remain highly subjective, as demonstrated by the relatively high interobserver and intraobserver variability. This is especially true when confronted with the problem of steatosis severity quantification. According to Strauss et al [6], the mean interobserver and intraobserver agreement rates for the presence of steatosis are 72% and 76%, while for severity of the disease, an interobserver agreement of 47-59% and an interobserver agreement of 59-64% were obtained. The intraobserver agreement rate for severity of the disease is 55%-68%. To improve these results, several computer vision based solutions have been proposed [7-10].

A recent dominant trend in computer assisted medical image analysis is the design of computer aided diagnosis systems (CAD) [11]. Such a system consists of an autonomous or semi-autonomous diagnosis procedure, obtained by methodologies developed in the field of pattern recognition [12-15]. The most important factors determining the performances of a CAD system are the selection of features and the selection of the classifier.

The most conspicuous image feature generated by accumulation of fat in the liver is the increase of the parenchyma brightness, as a result of the higher echogenicity of the fat cells. A related feature is the posterior attenuation (PA), also called deep attenuation, consisting of a progressive decrease of the liver brightness from surface to bottom and a reduced definition of the diaphragm. The average brightness and the PA in a selected region of interest (ROI) are used in most CAD systems for steatosis evaluation found in the literature.

Fat accumulation in the liver also affects the contrast of the vessels, since it diminishes the acoustic impedance between the parenchyma and the vessel walls. Vessels appear to be dilated and with blurred contours. Such changes may be characterized by means of image texture descriptors. Texture features include first order texture parameters, computed from ROI histograms [16], wavelet transform coefficients [17] and co-occurrence tensors [17]. First order texture parameters are simple to compute and have proved to be useful [16], although the spatial information is lost. This is in contrast to wavelet or co-occurrence tensors.

A comparative study about the usefulness of PA and first order texture features was calculated from the image histogram by Lupşor et al [16]. In this study the steatosis degree in patients infected with VHC was evaluated and they found that PA is capable of discriminating better than first order statistics based features. Reported work was carried out on different types of groups of patients taking into account liver state; some were already diagnosed with fibrosis or Hepatitis C, which alter the liver tissue microstructures and implicitly the characteristics of the ultrasound images. This is the reason why comparison of various solutions proposed for steatosis detection and evolution stage assessment is difficult.

To classify the steatosis based on extracted features, several methods are available and have been tested in the literature. The most popular are the Bayesian classifier with Gaussian model, the Parzen window nonparametric classifier, the k Nearest Neighbour classifier (kNN), the random forests (RF), and the support vector machines (SVM). According to current literature, the SVM was the most successful in quantifying diffuse liver disorders [17].

The potential advantage of RF is that this type of classifier has intrinsic mechanism of feature selection thus it has the ability to work with a high number of characteristics without deteriorating its performances. RF considers at the level of every decision node a single feature which performs best among the available ones, according to a certain criterion, like Gini index or entropy. Additionally, the classification process by RF resembles well with the medical diagnosis procedure. Moreover, it calculates the variable importance. This can be used to select and rely on best features for classification. RF is one of the most accurate ensemble classifiers used at this moment in computer vision community

The aim of our study was to compare the performances of the SVM and RF classifiers in the assessment

of steatosis severity rating using ultrasound images. For the automatic classification we assembled the feature vectors called training vectors. The classifier developed an algorithm for mapping the feature vectors and used training vectors for learning. SVM classifies well with a low number of data. RF belongs to the group of ensemble classifiers, being new in the field of computer vision and has not been used before in this domain.

Material and method

The study group consisted of 120 consecutive patients diagnosed with steatosis or normal liver by conventional abdominal ultrasound, in a Gastroenterology out-patient department. The diagnosis of steatosis was established based on the increased US brightness (bright liver) of the liver at transabdominal ultrasound, as compared to the nearby kidney parenchima, accompanied or not by PA. Three level of severity of steatosis were established depending on the intensity of PA: mild (discrete attenuation), moderate (obvious attenuation), and severe steatosis (difficult or impossible to visualize posterior diaphragm). All patients were assessed by US and the liver was classified by the same expert, a senior in Gastroenterology and expert in abdominal US as normal or with mild, moderate or severe steatosis. In all patients, at least 2 pictures were stored, in transverse and longitudinal subcostal sections.

All the images were than processed using SVM and RF. Parameters used were the minimum $(\hat{n}_{LO})$ and maximum gray level values in the liver ROI $(\hat{n}_{UP})$, minimum $(\hat{m}_{LO})$ and maximum attenuation in the liver ROI $(\hat{m}_{UP})$, the median grey levels for liver ROI (Med_{GL}), the median gray levels for another ROI, being interactively selected for reference in fat-free parenchyma belonging to a kidney (Med_{GK}), the variance (VAR) in the ROI, the skewness (SKW) and the kurtosis (KRS). Our best experts' ratings were used as ground truth data. The classifiers were trained using cross-validation. There was 80% of data randomly selected for training and 20% for testing the classifier. This procedure was performed 20 times.

Computer vision methods were used for automatic evaluation of liver steatosis from US images. We implemented a robust method from computer vision to compute the PA. We used the OpenCV library. For SVM classification Rapidminer v5.3 was used.

The study was approved by the local Ethics Committee.

According to usual practice, we extracted a set of image features from a user defined rectangular ROI (fig 1). The first feature we extracted in order to characterize the overall brightness of the ROI is the median. Compared to the mean value, the median is more robust to the presence of outlier samples within the measurement window, since $\hat{m}_i = \arg\min \sum_k |\hat{m}_i - y_k|^i$ (1) with $\hat{m}_1$ being the median and $\hat{m}_2$ the mean. The mean is much more sensitive to outlier samples, which influence the estimate with a weight which increases with the difference to the estimate. This is why, if the mean is to be used, the ROI should be selected much more carefully, to avoid inclusion of big vessels or of the diaphragm. The median of the ROI can be computed very fast from the histogram. Considering the normalized histogram, $h(k)$, the median is $\hat{m}_1 = k \mid \quad h(k-1) < 0.5, \quad h(k) \geq 0.5$ (2).

The second feature used in this work is the PA. To find this feature, we computed the brightness profile curve generated from the defined ROI. Each point on the curve was generated by averaging the image along its line: $C(k) = \sum_{j \in ROI} I(j,k) / \sum_{j \in ROI} 1$ (3). The brightness profile of a typical ROI is illustrated in figure 1. It can be seen that, in spite of the heavy smoothing, the curve still has a high degree of irregularity as well as a high degree of nonlinearity. Ribeiro et al [17] defined the PA as the slope of the line which "best" fits the curve. The best fit is obtained through linear regression, $PA = \arg\min_a \sum (ak + b - f(k))^2$ (4). Again, the least squares fit used was not robust to the presence of outlier data, as previously pointed out, for the case of the overall brightness characterization. For the same reason, we used the median estimator again, although not by dropping the squaring up operation in the last equation. Instead of that, we used an algorithm inspired from the RANSAC [18]. Moreover, to address the nonlinear character of the brightness profile, we fitted the curve with two lines. In this way, we obtained two slopes and two intercept parameters and subsequently studied the relevance of all these parameter for steatosis severity classification. We performed two robust regressions, namely one from the upper part, containing 30% of the ROI and

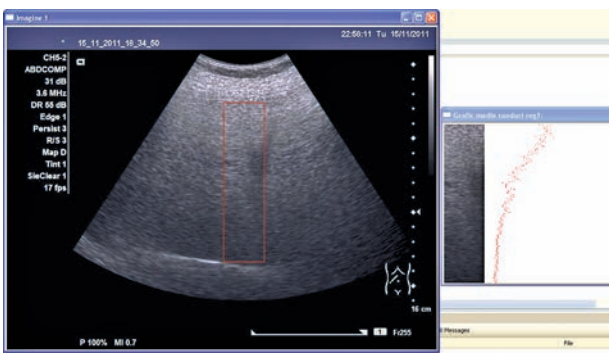

Fig 1. Region of interest and profile curve (red)

one from the lower part, which contains the rest of the curve. Further, we computed two PA coefficients and two intercept values, corresponding to robust estimates of the minimum gray level and maximum gray level. Minimum and maximum signal values are notoriously sensitive to noise and outliers, much more than the mean value, and our robust regression method dealt effectively with the problem.

To obtain estimates that are robust from the line parameters, described by the next equation: $y = mx + n$, (5) in the spirit of Random Sample Consensus (RANSAC), we formed sets of points of minimal size required to find estimates, for *m* and *n*. That is we formed sets of pairs of points, separated by *t* lines, a parameter of the method which balances the number of possible pairings and the effect of noise. A small value of *t* introduces too much quantization noise, while a too large one restricts the number of pairs of points. Its value is not critical and was set in all experiments to 20 lines. Unlike the original RANSAC algorithm, we did not use random sampling. Instead, we formed all pairs we could with a certain value of *t*. More minimal size samples could be obtained by using multiple values for *t*, but this option was not investigated.

A safe assumption is to consider that at least half of the minimal sets are free from outliers. Consequently, we defined our estimates by the following equations: $y_k = k, \quad x_k = C(k) \quad y_k^t = k + t, \quad x_k^t = C(k+t)$ (6). In equation (6), we used t=20 for all experiments reported in the paper. For each pair of points, by using equation (6), we found a candidate solution, (m_k, n_k), with $m = \Delta x_k / \Delta y_k$, (7) and $n = x_k + m * y_k$, (8). Then candidate parameters for best fit of the line was defined as, $\hat{m} = \arg\min \sum_k |\hat{m} - m_k| \quad \hat{n} = \arg\min \sum_k |\hat{n} - n_k|$ (9) which are known to be the medians of candidate solutions.

Using the robust line fit, for the upper part and the lower part of the brightness profile *C*(*k*), is illustrated in figure 2. By using this we extracted the minimum $(\hat{n}_{LO})$ and maximum gray level values in the ROI $(\hat{n}_{UP})$, the minimum $(\hat{m}_{LO})$ and maximum attenuation in the ROI $(\hat{m}_{UP})$.

Also, we computed the median grey levels for liver ROI (Med_{GL}). Further, we computed the median gray levels for another ROI, being interactively selected for reference in fat-free parenchyma belonging to a kidney (Med_{GK}). Using the histogram of the ROI we computed the variance (VAR), skewness (SKW) (10) and the kurtosis (KRS) (11).

$$skw = \frac{\sum_{i=1}^{n}(x_i - \bar{x})^3 p(x_i)}{(\sum_{i=1}^{n}(x_i - \bar{x})^2 p(x_i))^{3/2}} \quad (10),$$

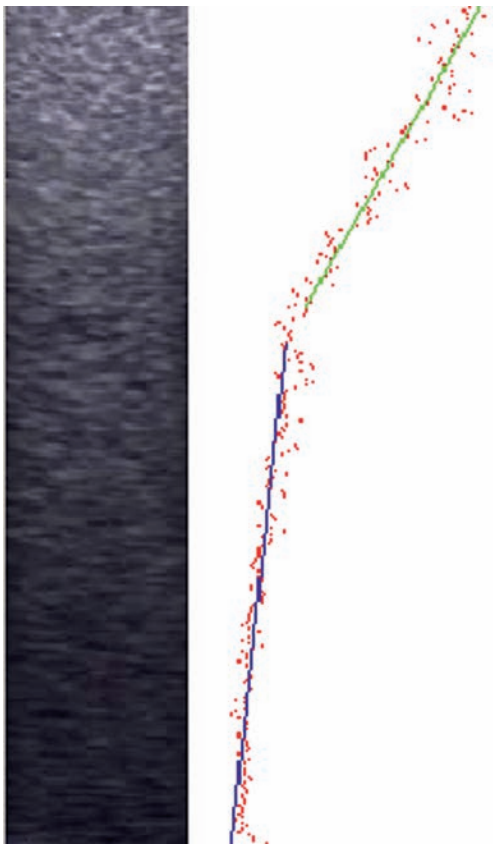

Fig 2. Regression fitting using two lines

$$krs = \frac{\sum_{i=1}^{n}(x_i - \bar{x})^4 p(x_i)}{(\sum_{i=1}^{n}(x_i - \bar{x})^2 p(x_i))^2} \quad (11).$$

To classify the severity levels of steatosis we considered four classes: absent, mild, moderate, and severe.

We implemented two versions of RF. The first version classified using all four classes simultaneously for decision. Each node of the Random forests was improved so that it extracted the minimum value of Gini index of the split data taking into account all the classes. The second version of the RF classifier (fig 3) used four successive dichotomies. The theoretical reason in considering this version is that discrimination between two classes is assumed to be feasible with simpler shapes of class borders. The first dichotomy split the data into liver with no steatosis and liver with steatosis. In the second step from the liver with steatosis set, the mild steatosis was extracted. Next the dichotomy between moderate and severe steatosis was used. Since in our previous work [10], the RF classifier using successive dichotomies performed best, we present here only the results of this classifier.

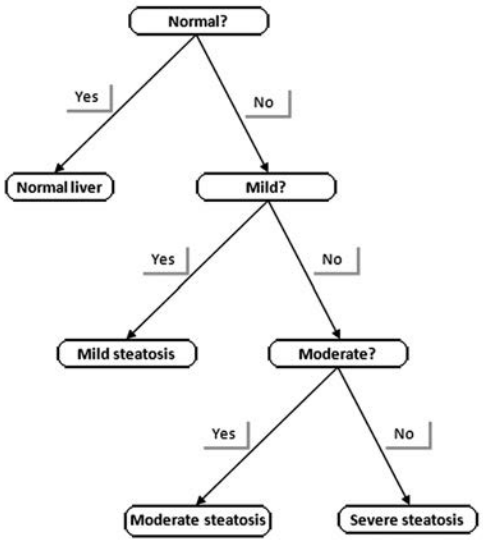

Fig 3. Dichotomy classification

The SVM classifier used for comparison reasons in this paper is a binary classifier. In its basic form, SVM maps the data into two classes by building hyperplanes. The hyperplane that splits the samples at a largest possible margin from support vectors of both classes is selected. To cope with more complex data, which are not linearly separable, the data vectors are mapped on a higher dimensional space, by the so called kernel trick. SVM classifiers are known for their ability to generalize well from low training sample sizes.

The main measure of performance and comparison was the accuracy.

For a successive dichotomy classifier, the Probability of error can be computed as $P_{et} = P_1 P_{e1} + P_2(P_{e1} + P_{e2}) + (P_3 + P_4)(P_{e1} + P_{e2} + P_{e3})$ (12) where P_i, and P_{ei} are prior class probabilities and respectively the error probabilities of the three binary classifiers in figure 3.

The accuracy of the classifier is defined as: A=(TP+TN)/(TP+TN+FP+FN) (13) where TP is the value of true positives, TN gives the number of true negatives, FP are the false positives and FN the false negatives.

The accuracy is related to the probability of error by the equation: $A=(1-P_{et})*100\%$ (14).

Results

The 120 patients included in our study had at abdominal US, normal liver (10 cases) mild steatosis (70 cases), moderate steatosis (33 cases) and severe steatosis (7 cases).

In the first set of experiments, we used for both classifiers the same set of nine features previously mentioned. The results of the SVM classifier are shown in Table I, while the results of the RF classifier are shown in Table II.

In a second set of experiments, we performed feature selection, guided by the variable importance index given by the RF classifier (table III). The best results of our

Table I. Support Vector Machines dichotomy classification

Classification	Healthy versus steatosis	Mild versus moderate + severe steatosis	Moderate versus severe steatosis
Minimum classification rate	91.67	70.91	82.5
Maximum classification rate	91.67	72.73	82.5
Standard deviation	0.0	0.7469	0.0
Median	91.67	72.73	82.5
Accuracy		60.51	

Table II. Random Forests dichotomy classification

Classification	Healthy versus steatosis	Mild versus moderate + severe steatosis	Moderate versus severe steatosis
Minimum classification rate	95.8	90.9	37.5
Maximum classification rate	100.0	100.0	100.0
Standard deviation	1.2927	3.1123	23.3941
Median	100.0	100.0	81.25
Accuracy		90.84	

Table III. Variable importance dichotomy

Variable importance [%]	
Maximum attenuation	3.45763
Maximum grey level	8.031634
Minimum attenuation	12.7997
Minimum grey level	6.656511
Liver median	42.49108
Median kidney	4.818146
Variance	13.20869
Skewness	3.766459
Kurtosis	4.770152

Table IV. Support Vector Machines dichotomy classification by maximum gray level values in the liver ROI ($\hat{n}_{UP}$), and median grey levels for liver ROI (Med_{gl})

Classification	Healthy versus steatosis	Mild versus moderate + severe steatosis	Moderate versus severe steatosis
Minimum classification rate	94.17	90.0	85.0
Maximum classification rate	94.17	91.82	85.0
Standard deviation	0.0	0.5343	0.0
Median	94.17	90.91	85.0
Accuracy		81.12	

Table V. Random Forests dichotomy classification maximum gray level values in the liver ROI ($\hat{n}_{UP}$), and median grey levels for liver ROI (Medgl)

Classification	Healthy versus steatosis	Mild versus moderate + severe steatosis	Moderate versus severe steatosis
Minimum classification rate	91.7	86.4	75.0
Maximum classification rate	100.0	100.0	100.0
Standard deviation	2.8120	4.2442	7.3392
Median	93.75	95.5	100.0
Accuracy		87.10	

Table VI. Support Vector Machines dichotomy classification classification by minimum attenuation in the liver ($\hat{m}_{LO}$) and median grey levels for liver ROI (Medgl)

Classification	Healthy versus steatosis	Mild versus moderate + severe steatosis	Moderate versus severe steatosis
Minimum classification rate	95.0	94.55	90.0
Maximum classification rate	95.0	96.36	92.50
Standard deviation	0.0	0.6871	1.1754
Median	95.0	95.45	90.0
Accuracy		87.78	

Tabel VII. Random Forests dichotomy classification by minimum attenuation in the liver ($\hat{m}_{LO}$) and median grey levels for liver ROI (Medgl)

Classification	Healthy versus steatosis	Mild versus moderate + severe steatosis	Moderate versus severe steatosis
Minimum classification rate	87.5	81.8	87.5
Maximum classification rate	100.0	100.0	100.0
Standard deviation	4.2488	4.5553	6.3802
Median	95.8	93.2	100.0
Accuracy		87.29	

experiments with the SVM and the RF classifiers using several feature sets are given in tables IV-VII.

From the tables, it can be seen that the accuracy of the SVM classifier is significantly higher after feature selection, while the results of the RF classifier are almost the same, although slightly lower.

This experiment gives the best result for the SVM classifier. As in the experiments using the pair of features consisting of ($\hat{n}_{UP}$) and Med_{GL}, the accuracy of the SVM is improved by feature selection, while the results of the RF classifier are poorer than those obtained with the full set.

After the best feature set selection the accuracy of the SVM classifier increased from 60.51 with the full set to 87.78, with the feature pair consisting of the minimum attenuation in the ROI ($\hat{m}_{LO}$) and the median grey levels for liver ROI (Med_{GL}). The accuracy of the RF classifier is best with the full feature set (90.84). These results are a confirmation of the theoretical feature selection mechanism embedded in the RF learning as an algorithm.

Discussion

RF is a relatively new ensemble classifier, which has not been used until now for steatosis severity evaluation. Since the SVM classifier proved to be the best for most feature sets in the recent work of Ribeiro et al [17], and because the SVM classifier was also used in most of the previous work for steatosis evaluation, we compared the performance of the RF with that of SVM. We concluded that RF based steatosis rating outperforms SVM classification, as well as human intraobserver and interobserver agreement rates.

In this work, the classifiers were trained on a set of 120 images, labeled by our best expert, unlike in the previous work, using biopsy data. While biopsy tests are undoubtedly more reliable than human evaluation, bi-

opsy data is scarce. Consequently, results of experiments based on biopsy data are drawn from rather small data sets, calling for caution in interpretation. It is especially difficult to ask for biopsy tests in normal patients, given the invasive nature of this test and the associated risks.

Comparison of the RF results with the full feature set and selected subsets, which did not contain texture data, confirmed that texture encodes valuable information for steatosis rating by visual analysis, in spite of the fact that the SVM classifier could not use effectively this information from human labeled images, in contrast with results on biopsy labeled samples. We believe that further work and classifier performance evaluation on larger datasets, possibly obtained by combining biopsy labeled images with expert or group of expert labeled images is worth following up.

Direct comparison of the classification accuracy of the proposed method with the results of the most relevant work on computer aided diagnosis of steatosis in the literature [7,16,17] is not possible, since these papers report only results of two class (steatosis versus normal) classification, in contrast with our study, targeting automatic quantification of the steatosis severity. Although our overall accuracy compared favorably with Nagy et al [7] and Lupşor et al [16] results and are similar to the Ribeiro et al [17] work, comparison is still problematic, given the different datasets and reference method used in our study. However, it is possible to assess the usefulness of the features used in literature in the present work.

The limit of this study is that the automatic classification uses expert medical assessment for the positive diagnosis, a subjective tool and not liver biopsy. On the other hand in clinical practice this is the algorithm used for diagnosis, and experience plays an important role in US assessment.

Conclusions. In this study the ability and accuracy of RF to classify well steatosis severity, without feature selection, were superior as compared to SVM.

Acknowledgment

This work was partially supported by the strategic grant POSDRU 107/1.5/S/77265 (2010) of the Ministry of Labor, Family and Social Protection, Romania, co-financed by the European Social Fund – Investing in people.

Conflict of interest: none

References

1. Farrell GC, Larter CZ. Nonalcoholic fatty liver disease: from steatosis to cirrhosis. Hepatology 2006; 43: S99-S112.
2. Adinolfi LE, Gambardella M, Andreana A, Tripodi MF, Utili R, Ruggiero G. Steatosis accelerates the progression of liver damage of chronic hepatitis C patients and correlates with specific HCV genotype and visceral obesity. Hepatology 2001; 33: 1358-1364.
3. Regev A, Berho M, Jeffers LJ, et al. Sampling error and intraobserver variation in liver biopsy in patients with chronic HCV infection. Am J Gastroenterol 2002; 97: 2614-2618.
4. Park SH, Kim PN, Kim KW, et al. Macrovesicular hepatic steatosis in living liver donors: use of CT for quantitative and qualitative assessment. Radiology 2006; 239: 105–112.
5. Bohte AE, van Werven JR, Bipat S, Stoker J. The diagnostic accuracy of US, CT, MRI and ^{1}H-MRS for the evaluation of hepatic steatosis compared with liver biopsy: a meta-analysis. Eur Radiol 2011; 21: 87-97.
6. Strauss S, Gavish E, Gottlieb P, Katsnelson L. Interobserver and intraobserver variability in the sonographic assessment of fatty liver. AJR Am J Roentgenol 2007; 189: W320-W323.
7. Nagy G, Gordan M, Vlaicu A, Mircea PA, Crişan D, Vălean S. Non-invasive evaluation of hepatic steatosis by ultrasound image analysis with simple brightness features and support vector machines. Acta Electrotehnica 2007; 4: 217-222.
8. Leandro G, Mangia A, Hui J, et al. Relationship between steatosis, inflammation, and fibrosis in chronic hepatitis C: a meta-analysis of individual patient data. Gastroenterology 2006; 130: 1636-1642.
9. Cao GT, Shi PF, Hu B. Liver fibrosis identification based on ultrasound images captured under varied imaging protocols. J Zhejiang Univ Sci B 2005; 6: 1107-1114.
10. Mihăilescu DM, Gui V, Toma CI, Popescu A, Sporea I. Automatic evaluation of steatosis by ultrasound image analysis. Conf Proc IEEE 2012 10th International Symposium on Electronics and Telecommunications 2012; ISBN 978-1-4673-1174-8; 2012: 311-314.
11. Sugimoto K, Shiraishi J, Moriyasu F, Doi K. Computer-aided diagnosis for contrast-enhanced ultrasound in the liver. World J Radiol 2010; 2: 215-223.
12. Duda RO, Hart PE, Stork DG. Pattern Classification 2nd edition. Wiley, 2000.
13. Bishop CM. Pattern Recognition and Machine Learning. Springer, 2006.
14. Cortes C, Vapnik V. Support-Vector Networks. Machine Learning 1995; 20: 273-297.
15. Breiman L. Random Forests. Machine Learning 2001; 45: 5-32.
16. Lupşor M, Badea R, Vicaş C, et al. Non-invasive Steatosis Assessment through the Computerized Processing of Ultrasound Images: Attenuation versus First Order Texture Parameters. International Conference on Advancements of Medicine and Health Care through Technology 2011; 2011: 184-189.
17. Ribeiro R, Tato Marinho R, Sanches JM. Global and local detection of liver steatosis from ultrasound. Conf Proc IEEE Eng Med Biol Soc 2012; 2012: 6547-6550.
18. Fischler MA, Bolles RC. Random sample consensus: a paradigm for model fitting and applications to image analysis and automated cartography. Communications of the ACM 1981; 24: 381-395.